

26 May 2010, 4:45 pm - 6:45 pm


## Earthquake Input Motions and Seismic Site Response in a Centrifuge Test Examining SFSI Effects

Henry B. Mason  
*University of California at Berkeley, Berkeley, CA*

Jonathan D. Bray  
*University of California at Berkeley, Berkeley, CA*

Katherine C. Jones  
*University of California at Berkeley, Berkeley, CA*

ZhiQiang Chen  
*University of California at San Diego, La Jolla, CA*

Tara C. Hutchinson  
Follow this and additional works at: <https://scholarsmine.mst.edu/icrageesd>  
*University of California at San Diego, La Jolla, CA*  
 Part of the [Geotechnical Engineering Commons](#)

---

See next page for additional authors

### Recommended Citation

Mason, Henry B.; Bray, Jonathan D.; Jones, Katherine C.; Chen, ZhiQiang; Hutchinson, Tara C.; Trombetta, Nicholas W.; Choy, Benjamin Y.; Kutter, Bruce L.; Fiegel, Gregg L.; Montgomery, Jack; Patel, Roshani J.; Reitherman, Robert D.; Bolisetti, Chandrakanth; and Whittaker, Andrew S., "Earthquake Input Motions and Seismic Site Response in a Centrifuge Test Examining SFSI Effects" (2010). *International Conferences on Recent Advances in Geotechnical Earthquake Engineering and Soil Dynamics*. 14.  
<https://scholarsmine.mst.edu/icrageesd/05icrageesd/session05/14>



This work is licensed under a [Creative Commons Attribution-Noncommercial-No Derivative Works 4.0 License](#).

This Article - Conference proceedings is brought to you for free and open access by Scholars' Mine. It has been accepted for inclusion in International Conferences on Recent Advances in Geotechnical Earthquake Engineering and Soil Dynamics by an authorized administrator of Scholars' Mine. This work is protected by U. S. Copyright Law. Unauthorized use including reproduction for redistribution requires the permission of the copyright holder. For more information, please contact [scholarsmine@mst.edu](mailto:scholarsmine@mst.edu).

---

**Author**

Henry B. Mason, Jonathan D. Bray, Katherine C. Jones, ZhiQiang Chen, Tara C. Hutchinson, Nicholas W. Trombetta, Benjamin Y. Choy, Bruce L. Kutter, Gregg L. Fiegel, Jack Montgomery, Roshani J. Patel, Robert D. Reitherman, Chandrakanth Bolisetti, and Andrew S. Whittaker



Fifth International Conference on

## Recent Advances in Geotechnical Earthquake Engineering and Soil Dynamics and Symposium in Honor of Professor I.M. Idriss

May 24-29, 2010 • San Diego, California

### EARTHQUAKE INPUT MOTIONS AND SEISMIC SITE RESPONSE IN A CENTRIFUGE TEST EXAMINING SFSI EFFECTS

**Henry B. Mason, Jonathan D. Bray and  
Katherine C. Jones**  
University of California at Berkeley  
Berkeley, CA-USA 94720

**ZhiQiang Chen, Tara C. Hutchinson  
and Nicholas W. Trombetta**  
University of California at San Diego  
La Jolla, CA-USA 92093

**Benjamin Y. Choy and Bruce L. Kutter**  
University of California at Davis  
Davis, CA-USA 95616

**Gregg L. Fiegel, Jack Montgomery and  
Roshani J. Patel**  
Cal Poly – San Luis Obispo  
San Luis Obispo, CA-USA 93407

**Robert D. Reitherman**  
CUREE  
Richmond, CA-USA 94804

**Chandranth Bolisetti and Andrew S.  
Whittaker**  
University of Buffalo  
Buffalo, NY-USA 14260

#### ABSTRACT

This paper describes the ground motion selection process and reports observed seismic site response and SFSI effects during a dynamic centrifuge test (Test-1). The centrifuge test is the first in a series of tests examining the effects of SFSI in dense urban environments. The objective of Test-1 is to examine SFSI effects for two structures that are located a significant distance apart and essentially isolated. The model structures represent a three-story building founded on spread footings and a nine-story structure founded on a three-story basement. The structures are sited on a dry, dense bed of Nevada Sand. The centrifuge model is subjected to a series of shaking events that represent near-fault and “ordinary” ground motions at a site in Los Angeles. Results show that site periods degrade as ground motion intensity increases with more pronounced degradation observed for near-fault ground motions as compared with ordinary ground motions. Additionally, the results indicate the importance of kinematic effects of embedded structures when considering SFSI effects.

#### INTRODUCTION

Dense urban environments are composed of city blocks that contain clusters of closely spaced buildings. During earthquake events, seismic waves propagate through the ground and interact with the foundations of the buildings, and the foundations then in turn interact with the superstructures. Soil-foundation-structure interaction (SFSI) is the term used to describe this phenomenon. It is common to split SFSI into two mechanisms – inertial interaction and kinematic interaction. The seismic-induced structural vibrations interacting with the foundation and soil cause inertial interaction. Kinematic interaction is caused by a stiff foundation in the soil, which causes the earthquake motions to deviate from those remote from the structure. SFSI has received much attention in the literature for individual structures. For example, Stewart *et al* (1998) summarize inertial interaction SFSI analysis methods for individual structures, which are repeated in FEMA-440 (FEMA 2006). Kim and Stewart (2003) provide a method for analyzing kinematic interaction SFSI effects.

Notably, for structures located in dense urban environments, the assumption of buildings being isolated from each other is invalid, and can lead to erroneous results. Therefore, consideration of the interaction of soils, foundations, and structures requires a more holistic approach. The phenomenon of adjacent structures interacting with each other through the ground supporting their foundations is commonly referred to as structure-soil-structure interaction (SSSI). Described in this paper is the first in a series of dynamic centrifuge tests designed to examine the effects of SSSI in dense urban environments. The paper summarizes the ground motion selection process for the test as well as observed geotechnical responses and SFSI effects. A primary objective of Test-1 is to examine SFSI effects for two structures that are located a significant distance apart and essentially isolated. A companion paper by Chen *et al* (2010) describes important structural details of Test-1 and observed structural response.

For earthquake engineering, the term free-field is often used, and we define it here to avoid confusion. The term is often reserved to describe sites located a significant distance from a

structure that causes wave scattering. Trifunac (1972) found that for an accelerometer to be considered in the free-field, it needs to be located a distance of at least an order of magnitude larger than the characteristic foundation dimension ( $B$ ). For Test-1, achieving a free-field condition by the Trifunac (1972) criteria is impossible given the size of the two structures and the size of the centrifuge soil container (i.e., the distance between the two models is 30 m, which is about three times the basement foundation size). Thus, the term “free-field,” as used in this paper, represents: “as free-field as possible given the modeling constraints.”

## LITERATURE REVIEW

In the early to mid-1970s, researchers investigated the effects of SSSI for shear walls and developed analytical expressions for foundation-level displacement amplitude and base shear. For example, Luco and Contesse (1973) found that SSSI effects need to be considered in the case of a small shear wall founded nearby a large shear wall. Wong and Trifunac (1975) conducted similar studies while examining the influence of non-vertically incident  $SH$ -waves and additional shear walls. Both studies concluded that SSSI effects are important when considering the normal frequency range of earthquake ground motions and the arrangements of structures found in dense urban environments. Simplifying assumptions required to develop the analytical procedures used in these studies included: the foundations are rigid and semi-circular; the soil is an elastic, homogeneous, isotropic half-space; the foundations are perfectly bonded to the soil; and the direction of the shaking is perpendicular to the plane of the building array.

Recent studies have employed analytical procedures with less restrictive assumptions. Qian and Beskos (1995) developed a boundary element method (BEM) model for considering interaction between adjacent, massless foundations. Mulliken and Karabalis (1998) developed a lumped mass model to consider ground-motion induced interactions between adjacent, massless foundations. More recently, other researchers have expanded the analytical methods to include pile foundations (e.g., Padron *et al* 2009). Other researchers (e.g., Wirgin and Bard 1996, Clouteau and Aubry 2001, Ghergu and Ionescu 2009) have considered how certain arrangements of typical structures in dense urban environments affect ground motion propagation. These researchers developed analytical tools for evaluating how seismic waves scatter in dense urban environments. These studies found that neglecting the wave scattering effects of the urban environment, and only considering free-field ground motions, can lead to erroneous results, especially for soft soil sites. Although these studies have developed important insights, their applicability in practice is hampered by the lack of observational data to validate the underlying theories and calibrate the analytical procedures.

## RESEARCH PROGRAM

As part of this research program, a series of geotechnical-structural centrifuge tests are being used to provide measure-

ments of SSSI effects. The results and insights gained from these tests will be used to evaluate current SSSI procedures. A goal is to then develop and calibrate improved, robust numerical models, which after calibration, can be used to generalize the results from the centrifuge experiments. Eventually, these generalized experimental results can be employed to develop simplified analytical procedures for incorporating SSSI effects into earthquake engineering hazard analyses.

The authors recently completed two centrifuge tests at the Center for Geotechnical Modeling (CGM) located at the University of California at Davis (UCD), which is one of fourteen Equipment Sites in the George E. Brown Jr. Network for Earthquake Engineering Simulation (NEES, [www.nees.org](http://www.nees.org)). Test-0 is used to develop an appropriate suite of earthquake ground motions for the project. Test-1 is the baseline test for the series. The goal of Test-1 is to understand the seismic response of two "isolated" structures that are located far enough apart that interaction is minimal. The structural models represent a three-story frame-braced structure on spread footings (MS1F\_SF80) and a nine-story frame-based structure on a three-story basement (MS3F\_B). Both Test-0 and Test-1 employ dry, dense Nevada Sand, which is placed at an initial relative density equal to approximately 80 percent.

Although centrifuge testing is widely accepted in geotechnical engineering, it is employed less in structural engineering research. Centrifuge experiments are invaluable for capturing effects in problems with materials that have stress-dependent engineering properties such as soil. Kutter (1995) states that the overarching objective of geotechnical centrifuge testing "...is to establish in a reduced scale model identical strength, stiffness and stress as that which exists in a much larger prototype." The size of the SSSI model is small (i.e., the actual measurements of the soil model used in Test-1 are 1652 mm long, 790 mm wide, and 536 mm thick). The prototype scale is what the increased gravitational field of the centrifuge creates. Test-0 and Test-1 were spun to achieve 55 g (i.e., a scale factor of 55). Length is scaled linearly with the scale factor; therefore, the dimensions of the soil deposit in prototype scale are 90.9 m long, 43.4 m wide, and 29.5 m thick. Table 1 provides a summary of important scaling factors for centrifuge testing. With properly scaled stresses in the soil model for a prototype soil deposit that is 29.9 m thick, realistic stress-dependent soil and SSSI responses can be captured in the centrifuge. All measurements in this paper are presented in prototype scale, unless otherwise noted.

Table 1. Important Scaling Factors Test-1

Quantity	Model Dimension/ Prototype Dimension
Density	1
Dynamic Time	1/55
Force	1/55 <sup>2</sup>
Frequency	55
Length	1/55
Mass	1/55 <sup>3</sup>
Period	1/55
Strain	1
Stress	1

## GROUND MOTION SELECTION

Centrifuge researchers have noted the importance of using a suite of realistic ground motions when studying dynamic phenomena (e.g., Kutter 1995). The use of simplified sinusoidal base motions with limited frequency content can overemphasize some results and underemphasize others; therefore, this project utilizes a suite of modified recorded earthquake ground motions. This section describes the details of the process used to select ground motion for this study.

Ground motions are selected from the PEER ground motion database ([www.peer.berkeley.edu](http://www.peer.berkeley.edu)) using design response spectra that were created following guidelines presented in the upcoming 2010 ASCE Standard 7. The 2008 probabilistic seismic hazard analysis (PSHA) tool developed by U.S. Geological Survey (<http://eqint.cr.usgs.gov/deaggint/2008/>) and deterministic seismic hazard analysis (DSHA) using the Next Generation Attenuation (NGA) relationships (Power *et al* 2008) are used. The project emphasizes near-fault, forward-directivity ground motions (Somerville *et al* 1997) because a dense urban area of Los Angeles was selected for the project location (N34.082 W118.224). “Ordinary” ground motions (i.e., those that occur at distances greater than 15 km from the site and do not show signs of forward-directivity) are also included as they too are potentially damaging and expected at the site. The design response spectrum is updated to include near-fault effects from reverse faults by using guidance from Somerville *et al* (1997), Spudich and Chiou (2008), and Huang *et al* (2008). The near-fault ground motions are defined based on their pulse-like qualities, as described by Bray *et al* (2009) and Baker (2007). Researchers at the CGM use the term “desired motions” to refer to the ground motions chosen at this stage.

The desired ground motions are converted into target ground motions that are safe to use in the centrifuge by filtering out potentially damaging frequencies (resonant frequencies of the centrifuge equipment). In the case of the UCD centrifuge, damaging frequencies are 5 Hz and 18 to 20 Hz. Additionally, for the more intense near-fault ground motions, frequency content in the range between 100 and 110 Hz were removed because this range excited another mode of the centrifuge equipment. A fifth-order high-pass Butterworth filter with a corner frequency of 10 Hz filters out the damaging first mode frequency band, and a fifth-order notch Butterworth filter with corner frequencies of 14 to 24 Hz filters out the damaging second mode frequency band. When necessary, a similar notch filter is also used for the 100 to 110 Hz frequency range. The resulting motion’s acceleration values are multiplied by 55 and the time values are divided by 55 to convert them to model scale to produce the target motions, which become the command motions for the shaker once converted to voltage.

A frequency-domain transfer function must be applied to the command motion to boost the high-frequency content (which the shaker has the most difficulty producing) and ensure that the achieved motion matches the target motion within a reasonable tolerance. For these purposes, a generic transfer func-

tion is usually employed based on experience with the centrifuge shake table. For this project, however, an initial calibration centrifuge test (Test-0) was performed to create a suite of target motions that match the achieved motions using three iterations of motion-specific transfer functions. This well-calibrated suite of eight ground motions have been used by other researchers performing tests at UCD at or near 55 g (Brandenberg, *personal communication*, 2009). Figure 1 shows the difference between the desired, target, and achieved motions obtained from Test-0 for two different motions. The JOS desired motion is well captured by its achieved motion; whereas the high-period energy of the SCS desired motion is reduced somewhat in its achieved motion.

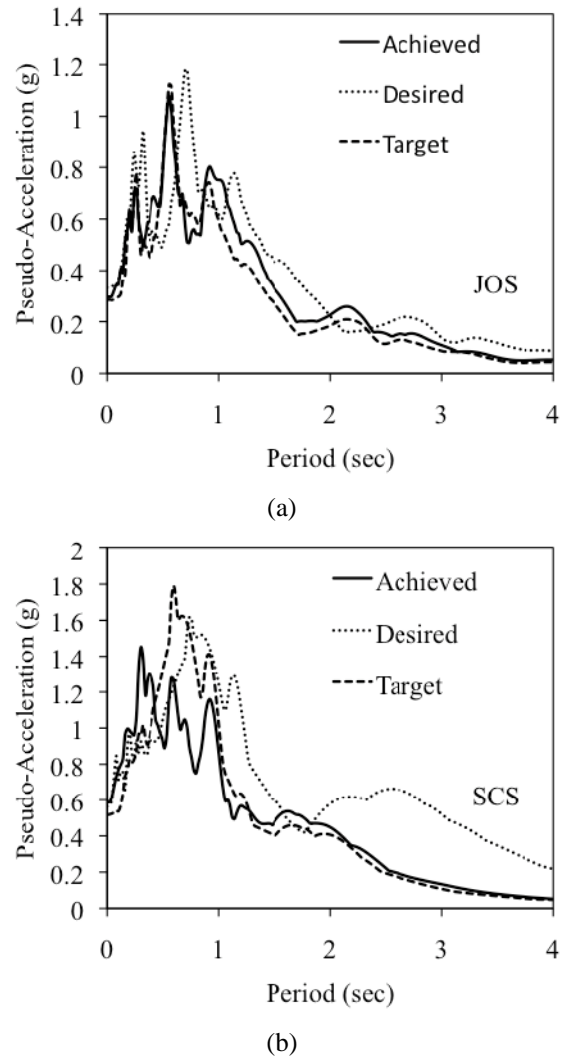


Fig. 1. Comparison of Different Types of Centrifuge Ground Motions: Desired, Target, Command and Achieved for the (a) 1992 Landers Joshua Tree motion; and (b) 1994 Northridge Sylmar Converter Station motion (5% damping)

The order of ground motions is chosen based on expected damage to the structures. In this case, an estimate of maximum ductility demand and associated number of inelastic cycles is

used as a proxy for tracking the expected structural damage (Chen *et al* 2010). A finite element model of the two structures used in Test-1 is created using the finite element program OpenSees (Mazzoni *et al* 2009). Each building responds differently; therefore, the maximum ductility demand is estimated for both structures and the maximum of these two values is used to determine the ground motion order. Strain gauges as well as cameras aimed at the hinges monitored the structural integrity of the beams during centrifuge testing. The damaged beams were replaced with new beams before damage became too severe to render the results meaningless (Chen *et al* 2010).

The OpenSees analyses require free-field surface acceleration-time series. Many of the Test-0 motions were found to be too intense, so they needed to be deamplified for use in Test-1. The equivalent-linear seismic site response program SHAKE2000 (Ordonez 2008) is used to help create the deamplified time series. Using the input base motions and recorded surface motions from Test-0, a deconvolved shear wave velocity profile is created such that the surface acceleration response spectra predicted by SHAKE2000 matches what is recorded in Test-0 within a reasonable margin. The Seed and Idriss (1970) modulus reduction (upper bound) and damping (lower bound) curves for sand are used and the unit weight is assumed to be  $16.7 \text{ kN/m}^3$ . The bedrock is assumed to be a linear half-space, and thus has no modulus reduction or damping. Figure 2 shows the deconvolved shear wave velocity profile and Fig. 3 shows the comparison between SHAKE2000 results and recorded Test-0 results for two motions.

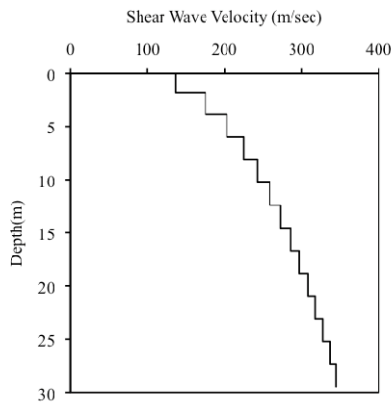
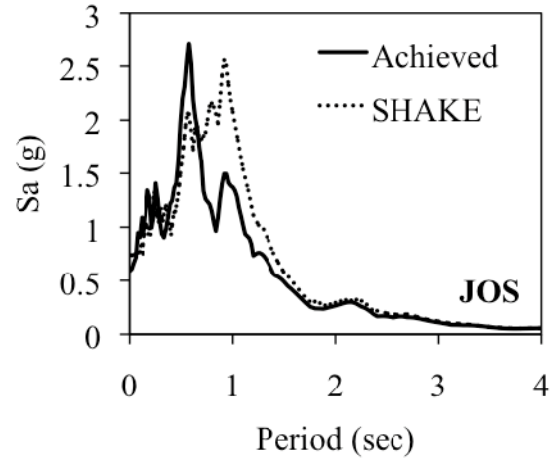


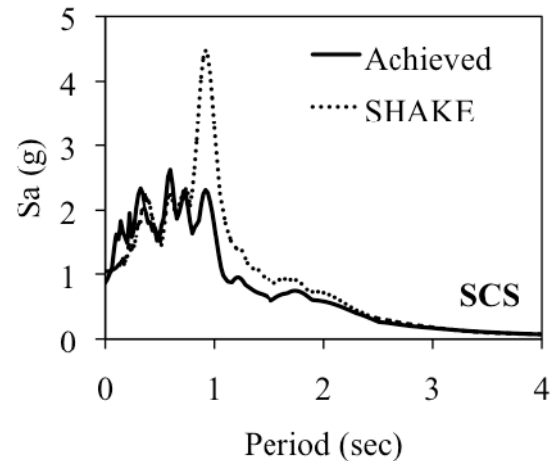
Fig. 2. Assumed Shear Wave Velocity Profile for SHAKE2000 Modeling

Input motions from Test-0 are scaled down using a linear scaling factor and then run through the calibrated SHAKE2000 model. The linear scaling factors are changed until the surface peak ground acceleration (*PGA*) predicted by SHAKE2000 match reasonably well. Another scaling factor is determined by dividing the *PGA* predicted by SHAKE2000 for the surface motion by the *PGA* recorded at the surface in Test-0 for the same motion. This scaling factor is then applied to the ground motions recorded in Test-0, and it is these ground motions that

are used for the OpenSees analyses. The decision was made to use free-field recorded ground motions for all OpenSees analyses primarily because this is common in structural engineering practice. Additionally, the hinge model used in the OpenSees analyses is simplified and not yet well calibrated; therefore, the predicted maximum ductility demand is a relative index of damage. For more details about the OpenSees analyses, see the companion paper by Chen *et al* (2010).



(a)



(b)

Fig. 3. Acceleration Response Spectra (5% damping) of Surface Motions Achieved in Test-0 versus the SHAKE2000 Predictions for (a) the 1992 Landers Joshua Tree Motion, and (b) the 1994 Northridge Sylmar Converter Station Motion

Table 2 shows the final order of the ground motions used in Test-1. Table 3 shows the *PGA* and peak ground velocity (*PGV*) recorded at the base for the ground motions, and their "type." The ground motions are divided into four bins based on whether the motion is near-fault (NF) or ordinary (Ord) and whether the motion is of lower-intensity (LI) or higher-intensity (HI). Motions are categorized according to these bins throughout this paper to help understand seismic response.



Table 2. Ground Motion Sequence for Ground Motions Used in Test-1

GM #	ID	Earthquake	Station
1	JOS_L_1	92 Landers	Joshua Tree 090
2	TCU_L	99 Chi Chi	TCU078 270 (E)
3	RRS	94 Northridge	Rinaldi R Sta 228
4	PTS	87 Sup Hills	Parachute T S 315
5	SCS_L_1	94 Northridge	Sylmar Conv Sta 052
6	LCN	92 Landers	Lucerne 260
7	JOS_L_2	92 Landers	Joshua Tree 090
8	SCS_L_2	94 Northridge	Sylmar Conv Sta 052
9	WVC_L	89 Loma Prieta	Saratoga WV Col 270
10	SCS_H	94 Northridge	Sylmar Conv Sta 052
11	JOS_H	92 Landers	Joshua Tree 090
12	WPI_L	94 Northridge	Newhall W Pico C 046
13	JOS_L_3	92 Landers	Joshua Tree 090
14	WPI_H	94 Northridge	Newhall W Pico C 046
15	PRI	95 Kobe	Port Island-Mod-79 m
16	TCU_H	99 Chi Chi	TCU078 270 (E)
17	WVC_H	89 Loma Prieta	Saratoga WV Col 270

Table 3. Important Test-1 Ground Motion Parameters

ID	Base PGA (g)	Base PGV (cm/s)	Type*
JOS_L_1	0.06	8.7	Ord, LI
TCU_L	0.11	11	Ord, LI
RRS	0.39	34	NF, HI
PTS	0.10	14	Ord, LI
SCS_L_1	0.18	20	NF, LI
LCN	0.26	44	NF, HI
JOS_L_2	0.06	8.8	Ord, LI
SCS_L_2	0.19	18	NF, LI
WVC_L	0.24	33	NF, HI
SCS_H	0.57	52	NF, HI
JOS_H	0.31	32	Ord, HI
WPI_L	0.37	44	NF, HI
JOS_L_3	0.06	8.4	Ord, LI
WPI_H	0.46	49	NF, HI
PRI	0.62	41	NF, HI
TCU_H	0.27	18	Ord, HI
WVC_H	0.33	46	NF, HI

\* Ord = ordinary, NF = near-fault, LI = lower-intensity, HI = higher-intensity

## TEST-1 EXPERIMENTAL SETUP AND RESULTS

### Model Description

The model is constructed with dry Nevada Sand that has a relative density ( $D_r$ ) of approximately 80%. The sand is uniformly graded, fine, and angular with a coefficient of uniformity ( $C_u$ ) equal to 1.06 and a mean grain diameter ( $D_{50}$ ) of 0.15 mm. Phalen (2003) found that Nevada Sand at relative density of 80% typically has a friction angle between  $37^\circ$  and  $42^\circ$ .

Nevada Sand is mined, and thus its soil properties change with each batch delivered to the CGM. Importantly, the maximum and minimum void ratios change; therefore, it is important to calculate relative density using lab data updated for each

batch. Cooper Labs performed tests on the Nevada Sand at the CGM on January 2, 2008. They determined that the specific gravity ( $G_s$ ) is 2.65, the minimum void ratio ( $e_{min}$ ) is 0.510, and the maximum void ratio ( $e_{max}$ ) is 0.748. Based on these soil properties, the target void ratio to obtain a relative density of 80% is 0.558, which corresponds to a target unit weight of 16.7 kN/m<sup>3</sup>. This target is used to calibrate the pluviator to create the model with a target relative density of 80%.

The soil instrumentation includes vertical arrays of accelerometers, which measure the achieved acceleration during the earthquake motions. The accelerometers are oriented in both the horizontal (in the plane of shaking) and vertical directions. Additionally, the soil contains arrays of displacement transducers. Figure 4 shows an elevation and plan view of the centrifuge model for Test-1 with all the sensor locations marked. This figure also shows the locations of the foundations and superstructures. For superstructure details, the reader should consult Chen *et al* (2010).

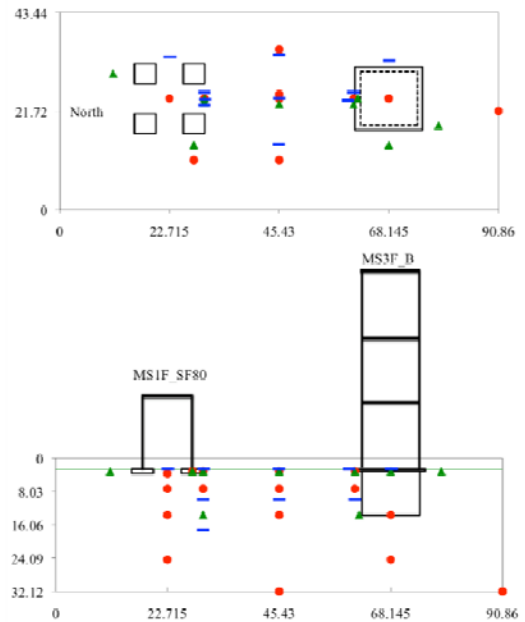


Fig. 4. Centrifuge Model Used for Test-1 (red circles = horizontal accelerometers; green triangles = vertical accelerometers; blue lines = displacement transducers). All measurements are in meters (prototype scale).

### Observed Seismic Site Response

Figures 5 and 6 show the free-field velocity-time series as a function of depth for the JOS\_L\_1 motion (lower-intensity, ordinary) and the SCS\_H motion (higher-intensity, near-fault), respectively. Figure 7 shows the velocity-time series for the LCN motion recorded at the base. The LCN motion is also a higher-intensity, near-fault ground motion though notably, it is somewhat less intense than the SCS\_H motion. Correspondingly, Figures 8, 9, and 10 show the free-field pseudo-

acceleration response spectra for the JOS\_L\_1, SCS\_H, and LCN motions, respectively.

Figures 5 and 6 demonstrate expected wave propagation characteristics; namely, the velocity-time series amplifies as it moves up through the soil column. Near-fault forward-directivity (FD) motions typically exhibit distinguishable velocity pulses (Bray *et al* 2009; Baker 2007). The SCS\_H motion shown in Fig. 6 contains some pulse-like characteristics, but the higher frequency content introduced by the transfer function required to replicate the long period aspects of this record makes its FD pulse less apparent. The FD pulse is better seen in the LCN motion shown in Fig. 7.

Figures 8, 9 and 10 present relevant pseudo-acceleration response spectra. For the less-intense motion (JOS\_L\_1), the *PGA* increases as the motion approaches and reaches the surface, and for the more intense SCS\_H motion, the *PGA* decreases as the motion moves up through the soil profile. For the medium-intensity LCN motion, the *PGA* generally increases as the motion propagates through the soil. At longer periods for the SCS\_H motion (i.e., larger than 0.5 sec), the spectral values increase as the motion propagates to the surface, which is contrary to what is observed for shorter period responses.

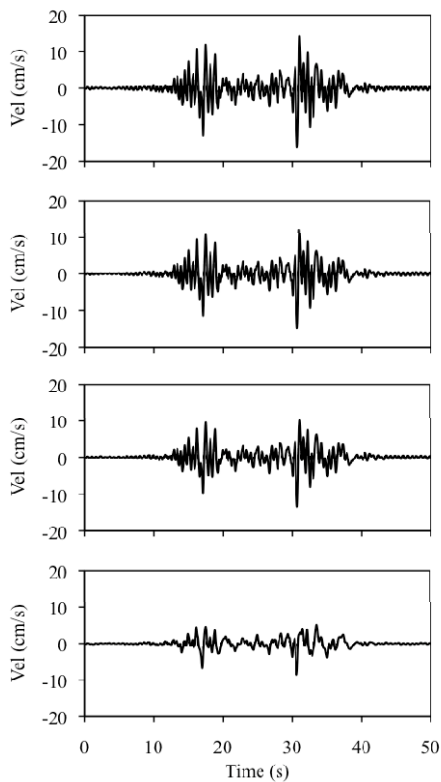


Fig. 5. Velocity-Time Series in the Free-field as a Function of Depth (Bottom to Top: Base Elevation, Basement Elevation, Sixth-Depth Elevation, Surface Elevation) for JOS\_L\_1

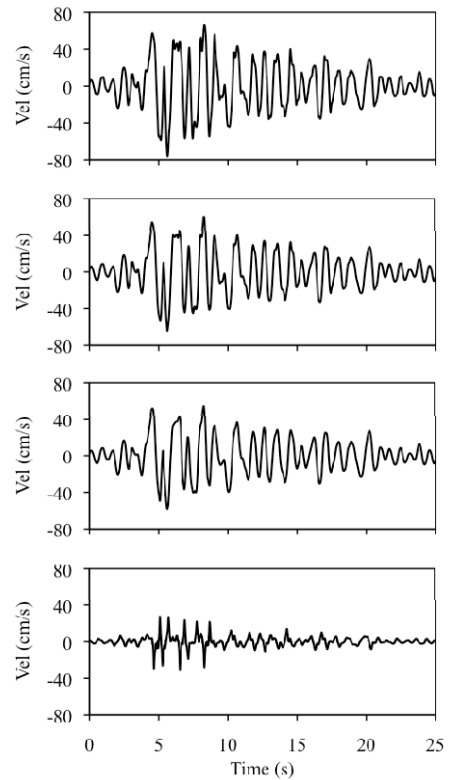


Fig. 6. Velocity-Time Series in the Free-field as a Function of Depth (Bottom to Top: Base Elevation, Basement Elevation, Sixth-Depth Elevation, Surface Elevation) for SCS\_H

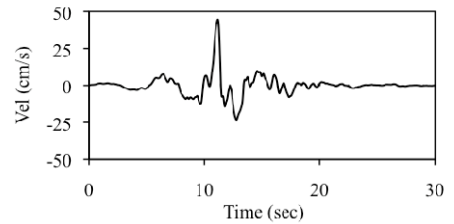


Fig. 7. Velocity-Time Series in the Free-field Recorded at the Base for LCN

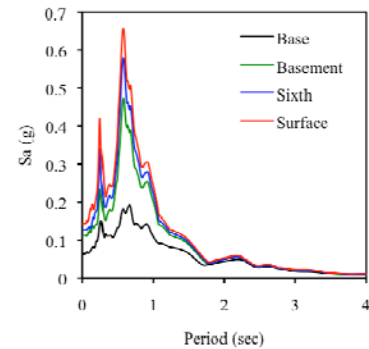


Fig. 8. Free-Field Acceleration Response Spectra (5% Damping) for the JOS\_L\_1 Motion at Base, Basement, Sixth-Depth, and Surface Elevations



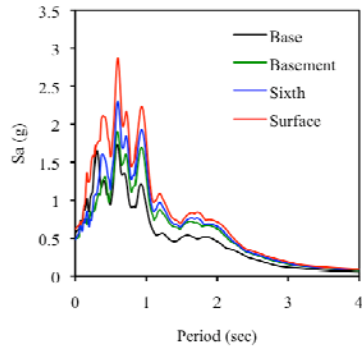


Fig. 9. Free-Field Acceleration Response Spectra (5% Damping) for the SCS\_H Motion at Base, Basement, Sixth-Depth, and Surface Elevations

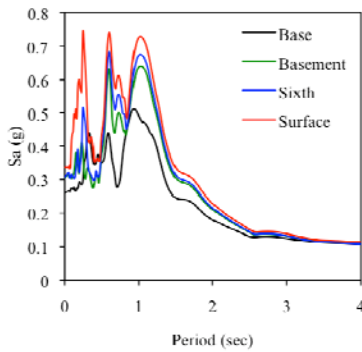


Fig. 10. Free-Field Acceleration Response Spectra (5% Damping) for the LCN Motion at Base, Basement, Sixth-Depth, and Surface Elevations

Figure 11 shows a plot of the recorded free-field surface *PGA* versus the input base *PGA* for the seventeen ground motions. These plots show how seismic site response changes as a function of ground motion intensity. For motions with a lower *PGA* at the base, a higher *PGA* is expected at the surface, due to the soil amplifying the motion. For more intense base motions, however, soil nonlinearity reduces the soil *PGA* amplification factor, and the surface motion can actually be less intense than the base motion due to the complex effects of material damping and other factors. A curve based on the intensity-dependent short-period amplification factors utilized in the 2006 International Building Code (IBC 2006) is also plotted on Fig. 6 for comparison. The 2006 IBC curve is developed using the  $F_a$  values found in Table 1613.5.3(1) of the code assuming site class D. The  $S_s$  values in this table are divided by 2.5 in order to “convert” them to input *PGA* values. Note that for values of *PGA* > 0.5 g, the 2006 IBC curve follows the 1:1 line, which is inconsistent with the results from other studies that indicate that soil nonlinearity should continue to reduce the short-period site amplification factors with increasing ground motion intensity (e.g., Seed *et al* 1997).

Figure 12 shows a plot of the recorded free-field surface *PGV* versus the input base *PGV* for the seventeen ground motions used in Test-1. *PGV* has been recognized as an important

ground motion parameter when considering near-fault, forward-directivity ground motions (e.g., Bray *et al* 2009). *PGV* values generally fall between the 1:1 line and 2:1 line. Additionally, a curve created using guidance from the 2006 IBC is plotted on this figure. The 2006 IBC curve is developed using the  $F_v$  values found in Table 1613.5.3(2) of the code assuming site class D. The  $S_v$  values in this table are converted to *PGV* by multiplying them by a factor of 100 cm/sec-g (i.e.,  $S_v = 0.1$  g converts to *PGV* = 10 cm/sec). This scaling factor is developed by converting the  $S_v$  value – which represents a spectral acceleration value at 1 sec – to a spectral velocity ( $S_v$ ) value at 1 sec and then dividing by an  $S_v$ /*PGV* ratio of 1.65 as suggested by Newmark and Hall (1982). Examining Fig. 12, it can be seen that the 2006 IBC curve and the data recorded in Test-1 are in good agreement, though on average, the 2006 IBC curve is slightly conservative.

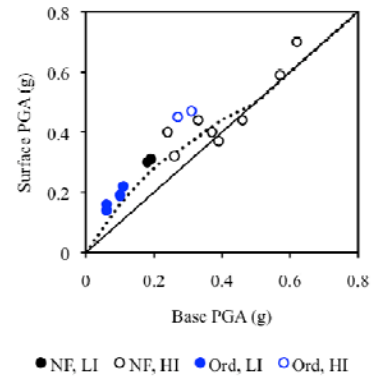


Fig. 11. PGA Recorded at the Surface (Free-Field) versus PGA Recorded at the Base for Test-1 Motions Divided into Ground Motion Bins. Dotted Line Represents the Line Creating Using 2006 IBC Guidance (IBC 2006).

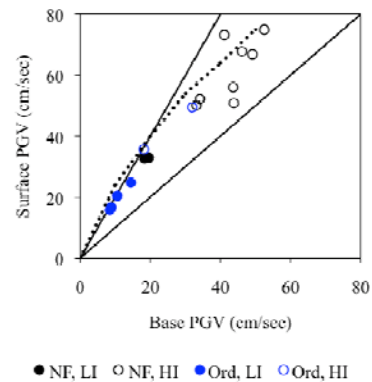


Fig. 12. PGV at the Surface (Free-Field) versus PGV at the Base for Test-1 Motions Divided into Ground Motion Bins. Dotted Line Represents the Line Creating Using 2006 IBC Guidance (IBC 2006).

Figure 13 shows the ratio of spectral ordinates between the surface and the base for the free-field case. The site period ( $T_s$ ) of the soil can be estimated based on the peaks in this figure.

With the exception of the near-fault, lower-intensity ground motion bin, this figure portrays expected response. Namely, the site period increases as the ground motions become more intense. This effect is referred to as a "degrading site period," and it is caused by soil nonlinearity. Ignoring interaction between the shaking apparatus and the specimen, the one-dimensional site period ( $T_s$ ) can be estimated as  $4H/V_s$ , where  $H$  is the thickness of the soil deposit and  $V_s$  is its equivalent-shear wave velocity, which is strain-dependent. As the soil is strained cyclically, its dynamic stiffness decreases, which increases the site period.

The site period degrades on average more for the near-fault ground motions as compared to the ordinary ground motions. This response is due to the intense pulse-like quality of the near-fault motions, which pushes the soil farther into the non-linear regime. The peak values of the ratio of spectral ordinates also decrease with increasing intensity, and are lower for the near-fault motions versus the ordinary motions. This is the same response shown in Fig. 11. It should be noted that the exceptional ground motion bin (NF, LI) contains only two motions, which are the same ground motions performed at the same intensity (SCS\_L\_1 and SCS\_L\_2). Therefore, the peak in response observed at the low period ( $T_s = 0.17$  sec) for the NF, LI bin is likely not indicative of a larger, more representative suite of lower-intensity, near-fault ground motions. In addition, it is noted that the NF, LI curve is tri-modal, and that the longer-period spike (at a period of around 0.9 sec) follows the expected trend.

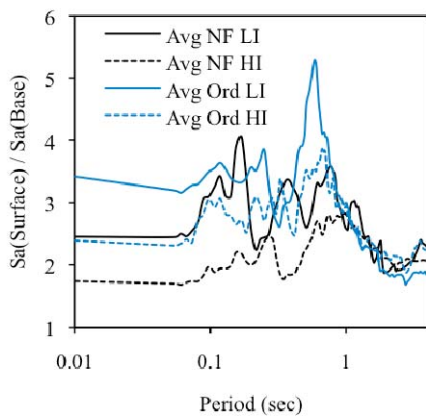


Fig. 13. Ratio of 5% Damped Spectral Acceleration Ordinates (Surface/Base) for Four Different Bins of Ground Motions for the Free-Field Case

### Soil-Foundation-Structure Interaction

In this paper, SFSI effects of the two "isolated" structures are examined by using velocity-time records measured in the soil adjacent to structures and in the free-field. Figures 14 and 15 show the velocity-time records as a function of depth for the soil accelerometers located adjacent to the basement of the MS3F\_B structure for the JOS\_L\_1 and SCS\_H motions, re-

spectively (refer to Fig. 4 for instrumentation plan). Figures 14 and 15 can be compared to Figs. 5 and 6 to assess kinematic interaction effects due to the 3-level basement foundation of Structure MS3F\_B.

Examining Figs. 14 and 15, one may observe that the characteristics of ground shaking are similar at all depths within the soil but noticeably different than those of the input base motion. The velocity-time records are similar in shape and amplitude for both the lower-intensity, ordinary JOS\_L\_1 motion and the higher-intensity, near-fault SCS\_H motion. There are also subtle yet discernable differences in the amplitude of the free-field velocity-time records (Figs. 5 and 6) and the velocity-time records measured near structures (Figs. 14 and 15). The ground shaking at the surface of the soil adjacent to the structure with the relatively stiff embedded basement is largely controlled by the shaking characteristics of the basement. Further, the shaking measured next to the basement is different than that measured in the free-field.

Stewart (2000) notes that kinematic interaction is most pronounced at higher frequencies, and thus *PGA* may be a good indicator of the amount of kinematic interaction observed. Table 4 presents *PGA* values at different soil depths for both the free-field and near-field cases. Additionally, this table contains values of the ratio between the near-field and free-field *PGA*. Note that near-field, in this case, refers to a location directly adjacent to the structure. As observed in the velocity-time series, the kinematic interaction effects are less pronounced for the lower-intensity JOS\_L\_1 motion. For the SCS\_H motion, the *PGA* is slightly amplified near the surface for the near-field case. However, the *PGA* is significantly deamplified for the near-field motion recorded at the bottom of the basement compared to the free-field, which is expected.

It is easier to distinguish near-fault effects on velocity-time records, which is why they are the preferred in this paper. However, since kinematic interaction is more pronounced at high-frequencies, the acceleration-time records are useful to compare. There is a practical difficulty with this approach, however. Because of the higher-frequency content of the acceleration-time series, it is harder to distinguish subtle differences by eye. An alternative is to use the acceleration response spectrum. Figures 16 and 17 show the acceleration response spectra for the JOS\_L\_1 motion and the SCS\_H motion, respectively. From these acceleration response spectra, it can be seen that the SFSI effects are more pronounced at lower periods, especially for the surface motion. The SCS\_H motion shows more SFSI effects than the JOS\_L\_1 motion across a wider period range. Additionally, the SCS\_H motion shows SFSI effects at the bottom of the basement, whereas the JOS\_L\_1 motion does not. These findings are in line with findings obtained by examining the velocity-time records, as discussed earlier.

Importantly, representative buildings in the Los Angeles basin are normally low-rise to mid-rise with periods between 0.2 and 2.5 sec (Ganuzza 2006). Therefore, from Figs. 16 and 17, we expect SFSI effects to be important for the Los Angeles

building stock – especially the lower-rise buildings. This observation matches previous experience – which indicates that stiff (lower-period) structures founded on soft soil experience the most significant SFSI effects (Stewart *et al* 1998).

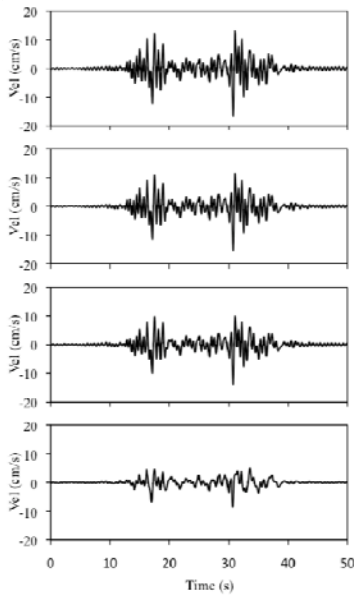


Fig. 14. Velocity-Time Series in the Near-Field (Adjacent to MS3F\_B) as a Function of Depth (Bottom to Top: Base Elevation, Basement Elevation, Sixth-Depth Elevation, Surface Elevation) for JOS\_L\_1

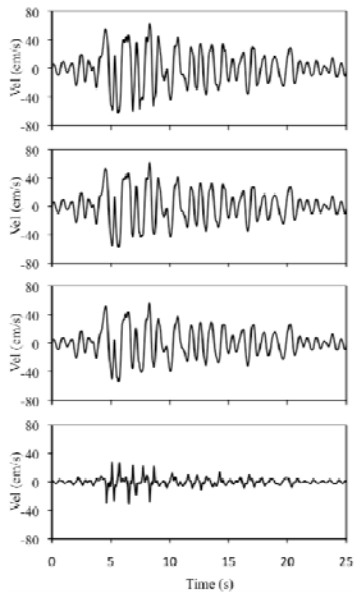


Fig. 15. Velocity-Time Series in the Near-Field (Adjacent to MS3F\_B) as a Function of Depth (Bottom to Top: Base Elevation, Basement Elevation, Sixth-Depth Elevation, Surface Elevation) for SCS\_H

Table 4. Free-Field versus Near-Field PGA Response (JOS = JOS\_L\_1, SCS = SCS\_H; all PGA in g)

Depth	Free-field		Near-field		Near-field/ Free-field	
	JOS	SCS	JOS	SCS	JOS	SCS
Surface (0 m)	0.14	0.61	0.14	0.64	0.98	1.04
Sixth-depth (4.9 m)	0.13	0.48	0.13	0.51	1.01	1.06
Basement (11.1 m)	0.11	0.49	0.11	0.44	0.99	0.90

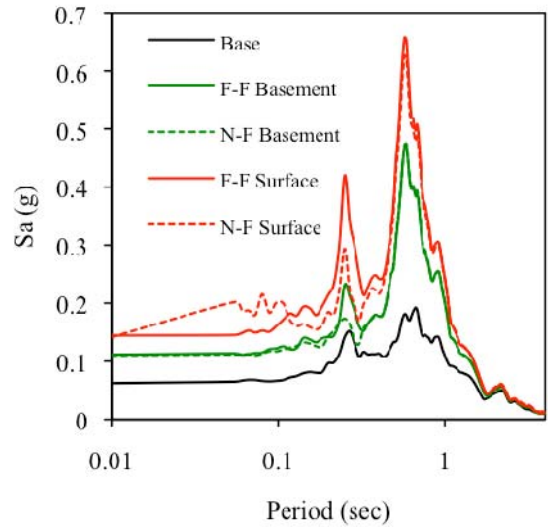


Fig. 16. Acceleration Response Spectrum (5% Damping) for the JOS\_L\_1 Motion Comparing Motions Recorded in the Free-Field (F-F) versus Motions Recorded in the Near-Field (N-F).

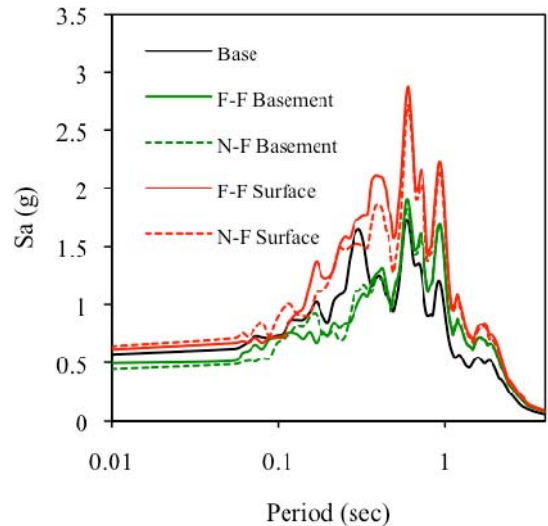


Fig. 17. Acceleration Response Spectrum (5% Damping) for the SCS\_H Motion Comparing Motions Recorded in the Free-Field (F-F) versus Motions Recorded in the Near-Field (N-F).

## CONCLUSIONS

Soil-foundation-structure interaction and structure-soil-structure interaction effects in dense urban environments with closely spaced structures are being investigated. In this paper we discuss the ground motion selection procedure for the testing program and preliminary results from a recently completed centrifuge test (Test-1). The importance of the ground motion selection process for centrifuge testing cannot be overemphasized as the input ground motions greatly impact the seismic site response, the dynamic response of the structures, and resulting SFSI/SSSI effects. Many previous centrifuge testing programs have employed sine waves or a limited number of commonly used earthquake motions. Through this study, a relatively large set of near-fault and ordinary ground motion records have been developed which can be used in this and other centrifuge studies at the UCD NEES Equipment Site.

Using these results, seismic site response is studied. As expected, the site period lengthens as the input ground motions become more intense and soil nonlinearity increases. Greater lengthening of the site periods are observed for the intense near-fault ground motions relative to the ordinary ground motions. Additionally, amplification of the ground motion as it propagates from the base to the surface decreases as intensity of the ground motion increases.

Preliminary near-field versus far-field results are also analyzed in this paper. The differences between ground response in the near-field of the nine-story structure and the free-field are investigated. Comparing the near-field and free-field ground response highlights the kinematic interaction effects caused by the deeply embedded basement. The ground shaking at the surface of the soil adjacent to the building with the embedded stiff basement was largely controlled by the shaking characteristics of the basement. Importantly, the shaking was different than that in the free-field. Thus, SSSI effects could be important when a smaller structure is situated adjacent to a larger structure with an embedded foundation.

In Test-2, the same two structures used for Test-1 will be placed adjacent to one another. This will more accurately mimic the location of two structures in a typical dense urban environment. A comparison of Test-1 and Test-2 will shed light on the differences between SFSI for isolated structures and SSSI for the more realistic case of adjacent structures. The reader is encouraged to track the progress of this project at the project website: <http://www.nees-cityblock.org/>.

## ACKNOWLEDGMENTS

This material is based upon work supported by the National Science Foundation under Grant No. CMMI-0830331. Any opinions, findings, and conclusions or recommendations expressed in this material are those of the authors and do not necessarily reflect the views of the National Science Foundation. The authors gratefully acknowledge the assistance of the staff of the Center for Geotechnical Modeling at the Universi-

ty of California at Davis during the centrifuge testing. We would also like to acknowledge the significant contributions of our professional practice committee: Marshall Lew, Mark Moore, Farzad Naeim, Farhang Ostadan, Paul Somerville, and Michael Willford. Finally, we would like to thank Lijun Deng for his help with the MathCAD processing.

## REFERENCES

- Baker, J. W. [2007]. Quantitative classification of near-fault ground motions using wavelet analysis, *Bulletin of the Seismological Society of America*. 97(5): 1486-1501.
- Bray, J. D., A. Rodriguez-Marek, and J. L. Gillie [2009]. Design ground motions near active faults, *Bulletin of the New Zealand Society for Earthquake Engineering*. 42(1): 1-8.
- Chen, Z., T. C. Hutchinson, N. W. Trombetta, H. B. Mason, J. D. Bray, K. C. Jones, C. Bolisetti, A. S. Whittaker, B. Y. Choy, B. L. Kutter, G. L. Fiegel, J. Montgomery, R. J. Patel, and R. D. Reitherman [2010]. Seismic performance assessment in dense urban environments: evaluation of nonlinear building-foundation systems using centrifuge tests, *5<sup>th</sup> International Conference on Recent Advances in Geotechnical Engineering and Soil Dynamics*. May 24-29, San Diego, CA.
- Clouteau, D. and D. Aubry [2001]. Modifications of the ground motion in dense urban areas, *Journal of Computational Acoustics*. 9(4): 1659-1675.
- FEMA [2006]. *FEMA 440: Improvement of Nonlinear Static Seismic Analysis Procedures*. Applied Technology Council, Redwood City, California.
- Ganuza, E. A. B. [2006]. *Seismic Behavior of Hybrid Lateral-Force-Resisting Systems*. Master Thesis, Department of Civil, Structural and Environmental Engineering, the State University of New York at Buffalo.
- Ghergu, M. and I. R. Ionescu [2009]. Structure-soil-structure coupling in seismic excitation and "city effect," *International Journal of Engineering Science*. 47: 342-354.
- Huang, Y-N., A. S. Whittaker and N. Luco [2008]. Maximum spectral demands in the near-fault region, *Earthquake Spectra*. 24(1): 319-341.
- IBC [2006]. *International Building Code*. International Code Council, Country Club Hills, Illinois.
- Kim, S., and J. P. Stewart [2003]. Kinematic soil-structure interaction from strong motion recordings, *Journal of Geotechnical and Geoenvironmental Engineering*. 129(4): 323-335.

- Kutter, B. L. [1995]. Recent advances in centrifuge modeling of seismic shaking, *Proceedings: Third International Conference on Recent Advances in Geotechnical Earthquake Engineering and Soil Dynamics*. St. Louis, MO, Vol. III, Paper No. SOA8.
- Luco, J. E. and L. Contesse [1973]. Dynamic structure-soil-structure interaction, *Bulletin of the Seismological Society of America*. 63(4): 1289-1303.
- Mazzoni, S., F. McKenna, M. H. Scott, and G. L. Fenves [2009]. *Open System for Engineering Simulation User-Command-Language Manual*, version 2.0, Pacific Earthquake Engineering Research Center, University of California, Berkeley. <<http://opensees.berkeley.edu/>>.
- Mulliken, J. S. and D. L. Karabalis [1998]. Discrete model for dynamic through-the-soil coupling of 3-D foundations and structures, *Earthquake Engineering and Structural Dynamics*. 27: 687-710.
- Newmark, N. M., and W. J. Hall [1982]. *Earthquake Spectra and Design*. Earthquake Engineering Research Institute, Monograph 3, Oakland, CA.
- Ordonez, G. A. [2008]. *SHAKE2000: A Computer Program for the 1-D Analysis of Geotechnical Earthquake Engineering Problems*, User Manual, June 2008 version, <<http://www.shake2000.com/download/Manual.pdf>>
- Padron, L. A., J. J. Aznarez, and O. Maeso [2009]. Dynamic structure-soil-structure interaction between nearby piled buildings under seismic excitation by BEM-FEM model, *Soil Dynamics and Earthquake Engineering*. 29: 1084-1096.
- Phalen, J. D. (2003). *Physical Modeling of the Soil-Foundation Interaction of Spread Footings Subjected to Lateral Cyclic Loading*. M.S. Thesis, University of California at Davis.
- Power, M., B. Chiou, N. Abrahamson, Y. Bozorgnia, T. Shantz, and C. Roblee [2008]. An overview of the NGA project, *Earthquake Spectra*. 24(1): 3-21.
- Qian, J. and D. E. Beskos [1995]. Dynamic interaction between 3-D rigid surface foundations and comparison with the ATC-3 provisions, *Earthquake Engineering and Structural Dynamics*. 24: 419-437.
- Seed, H.B. and I. M. Idriss [1970]. *Soil Moduli and Damping Factors for Dynamic Response Analyses*, Report No. UCB/EERC 70/10, Earthquake Engineering Research Center, University of California, Berkeley.
- Seed, R. B., S. W. Chang, S. E. Dickenson, and J. D. Bray [1997]. Site-dependent seismic response including recent strong motion data, *Proceeding of the Special Session on Earthquake Engineering, XIV International Conference on Soil Mechanics and Foundation Engineering*, Sept. 6-12, Hamburg, Germany.
- Somerville, P. G., N. F. Smith, R. W. Graves, and N. A. Abrahamson [1997]. Modification of empirical strong ground motion attenuation relations to include the amplitude and duration effects of rupture directivity, *Seismological Research Letters*. 68(1): 199-221.
- Spudich, P. and B. S. J. Chiou [2008]. Directivity in NGA earthquake ground motions: Analysis using isochrones theory, *Earthquake Spectra*. 24(1): 279-298.
- Stewart, J. P. [2000]. Variations between foundation-level and free-field earthquake ground motions, *Earthquake Spectra*. 16(2): 511-532.
- Stewart, J. P., R. B. Seed, and G. L. Fenves [1998]. *Empirical Evaluation of Inertial Soil-Structure Interaction Effects*, Report No. PEER-98/07, Pacific Engineering Research Center, University of California, Berkeley.
- Trifunac, M. D. [1972]. Interaction of a shear wall with the soil for incident plane SH waves, *Bulletin of the Seismological Society of America*. 62(1): 63-83.
- Wirgin, A. and P-Y Bard [1996]. Effects of buildings on the duration and amplitude of ground motion in Mexico City, *Bulletin of the Seismological Society of America*. 86(3): 914-920.
- Wong, H. L. and M. D. Trifunac [1975]. Two-dimensional, antiplane, building-soil-building interaction for two or more buildings and for incident plane SH waves, *Bulletin of the Seismological Society of America*. 65(6): 1863-1885.